Antimitotic Antifungal Compound Benomyl Inhibits Brain Microtubule Polymerization and Dynamics and Cancer Cell Proliferation at Mitosis, by Binding to a Novel Site in Tubulin†

Kamlesh Gupta,‡ Jamie Bishop,§ Austin Peck,§ Julie Brown,§ Leslie Wilson,§ and Dulal Panda*,‡

School of Biosciences and Bioengineering, Indian Institute of Technology, Bombay, Mumbai India 400076, and Department of Molecular, Cellular, and Developmental Biology, University of California, Santa Barbara, California 93106

Received November 25, 2003; Revised Manuscript Received March 15, 2004

ABSTRACT: The antifungal agent benomyl [methyl-1-(butylcarbamoyl)-2-benzimidazolecarbamate] is used throughout the world against a wide range of agricultural fungal diseases. In this paper, we investigated the interaction of benomyl with mammalian brain tubulin and microtubules. Using the hydrophobic fluorescent probe 1-anilinonaphthalene-8-sulfonic acid, benomyl was found to bind to brain tubulin with a dissociation constant of 11.9 ± 1.2 μM. Further, benomyl bound to at a novel site, distinct from the well-characterized colchicine and vinblastine binding sites. Benomyl altered the far-UV circular dichroism spectrum of tubulin and reduced the accessibility of its cysteine residues to modification by 5,5′-dithiobis-2-nitrobenzoic acid, indicating that benomyl binding to tubulin induces a conformational change in the tubulin. Benomyl inhibited the polymerization of brain tubulin into microtubules, with 50% inhibition occurring at a concentration of 70−75 μM. Furthermore, it strongly suppressed the dynamic instability behavior of individual brain microtubules in vitro as determined by video microscopy. It reduced the growing and shortening rates of the microtubules but did not alter the catastrophe or rescue frequencies. The unexpected potency of benomyl against mammalian microtubule polymerization and dynamics prompted us to investigate the effects of benomyl on HeLa cell proliferation and mitosis. Benomyl inhibited proliferation of the cells with an IC_{50} of 5 μM, and it blocked mitotic spindle function by perturbing microtubule and chromosome organization. The greater than expected actions of benomyl on mammalian microtubules and mitosis together with its relatively low toxicity suggest that it might be useful as an adjuvant in cancer chemotherapy.

Benzimidazoles are widely used as antifungal agents in agriculture and as antihelminthic agents in veterinary and human medicine. Benomyl [methyl-1-(butylcarbamoyl)-2-benzimidazolecarbamate] (Figure 1) is a systemically active benzimidazole that is selectively toxic to fungi. It is used extensively as an agricultural fungicide against a wide range of fungal diseases affecting fruit trees and field crops and has been highly useful as a research tool in fungal cell biology (*1*−*3*). It inhibits fungal cell growth during mitosis of the cell cycle and has been thought to act selectively on fungal cell tubulin and microtubules (*1*, *4*). The selectivity of benomyl for fungal cells is believed to be due to its high affinity for fungal cell tubulin and its relatively low affinity for mammalian tubulin (*4*−*8*). For example, carbendazim, a major metabolite of benomyl, inhibited yeast tubulin polymerization potently ($IC_{50} \sim 4$ μM); however, a very high concentration of carbendazim ($IC_{50} \sim 1.3$ mM) was required to inhibit mammalian tubulin polymerization (*7*). Because

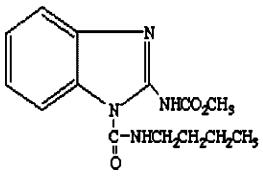

FIGURE 1: Structure of benomyl [methyl-1-(butylcarbamoyl)-2-benzimidazolecarbamate].

benomyl is a member of the benzimidazole class of compounds, several of which bind to the colchicine-binding site in tubulin, it has been suggested to bind weakly to the colchicine-binding site (*4*−*7*). In contrast, site-directed mutagenesis of the yeast *Saccharomyces cerevisiae* β-tubulin (*TuB1*) gene has indicated that the benomyl binding site may be located in the core of β tubulin, some distance from the colchicine site, which is thought to be at the interface between the α and β tubulins (*9*−*11*). The affinity of benomyl for mammalian-cell tubulin and the location of its binding site in the tubulin have not been determined experimentally.

The strongest evidence indicating that tubulin is the target for benomyl in fungal cells comes from studies in which specific mutations in the β-tubulin gene confer resistance or increased sensitivity to the compound (*11*−*19*). For example, a series of charged-to-alanine mutations that systematically

† This study was supported by a Fogarty International Research Grant TW05550 (to D.P. and L.W.), U. S. Public Health Service Grant NS13560 (to L.W.), and Department of Biotechnology Grant from the government of India to D.P.

* To whom correspondence should be addressed. Phone: 91-22-2576-7838. Fax: 91-22-2578-3480. E-mail: panda@iitb.ac.in.

‡ Indian Institute of Technology.

§ University of California.

10.1021/bi036112v CCC: $27.50
Published on Web 05/07/2004

altered the β-tubulin gene in the yeast *Saccharomyces cerevisiae* β tubulin produced both super-sensitivity and resistance phenotypes (*11*−*19*). The studies show that the 198−200 amino acid region of yeast β tubulin is involved in benzimidazole binding and that point mutations in this region lead to benzimidazole resistance (*11*−*15*). Specifically, point mutations that replace Glu_{198} with Ala, Val, or Gly or which replace Phe_{200} with Tyr reduce the affinity of benzimidazole for tubulin. However, very little is known at a mechanistic level how benomyl interacts either with mammalian- or fungal-cell tubulin. Further, while it has been assumed that the affinity of benomyl for mammalian tubulin is very weak, its binding to mammalian tubulin, its effects on mammalian microtubule polymerization and dynamics, and its antimitotic effects in mammalian cells have not been determined.

Microtubules are major structural components of the cytoskeleton of the cell and play important roles in cell motility, intracellular transport, mitosis, and many other cellular processes (*20*−*24*). They are dynamic polymers composed of α- and β-tubulin heterodimers. Microtubules are the targets of a variety of antimitotic drugs that inhibit mitosis in mammalian cells by interfering with the rapid dynamics of the spindle microtubules required for normal mitotic progression (*25*−*28*). Tubulin/microtubule-targeted antimitotic drugs are valuable for the treatment of cancer, as herbicides, as antifungal drugs, and as antihelminthic drugs (*25*−*29*). There are two characterized drug-binding sites in tubulin to which drugs that inhibit microtubule polymerization are thought to bind. One is the colchicine binding site in β tubulin, where drugs such as colchicine itself, podophyllotoxin, combreastatin, and curacin A, are thought to bind (*28*−*31*). The second is the Vinca-binding site, also thought to be in β tubulin, where the Vinca alkaloids, cryptophycins, and maytansinoids, among others, bind (*32*, *33*). Most of these drugs at relatively high concentrations act by inhibiting microtubule polymerization and, at relatively low concentrations, act by modulating the dynamics of the microtubules (*25*−*29*).

While tubulins are highly conserved proteins, there are significant species differences among the tubulins. These differences are responsible for the selectivity of drugs for tubulins from different species (*34*, *35*). The binding of benomyl to tubulin and its effects on microtubule polymerization and dynamics at a mechanistic level in fungal cells are poorly understood. Further, its effects on mitosis in mammalian cells and its interaction with mammalian tubulin and microtubules are essentially not known. In this paper, we examined the binding of benomyl to mammalian brain tubulin and the effects of the drug on mammalian tubulin polymerization and microtubule dynamics. We also examined the effects of benomyl on HeLa cell proliferation and mitosis. We find that benomyl does bind to mammalian brain tubulin but relatively weakly, with a K_d of 11.9 ± 1.2 μM. It binds to a site that appears to be distinct from that of colchicine and vinblastine. Interestingly, while the binding to brain tubulin itself is weak, it exerts a surprisingly strong effect on microtubule dynamics. We also find that benomyl does inhibit mammalian (HeLa) cell proliferation (IC_{50} = 5 μM) and that it inhibits mitosis by ~50% at a concentration of 15 μM. The results indicate that benomyl is selective for fungal tubulin and microtubules; it does indeed interact with mammalian tubulin and can exert effects on mammalian microtubule function that may be important in its toxicity or for its possible use in the treatment of cancer.

EXPERIMENTAL PROCEDURES

Materials. GTP,[1] pipes, colchicine, and vinblastine were obtained from Sigma (St. Louis, MO). Benomyl was obtained from Aldrich (Milwaukee, WI). ANS and fluorescent vinblastine (BODIPY FL-vinblastine) were obtained from Molecular Probes (Eugene, OR). Phosphocellulose (P11) was obtained from Whatman (Maidstone, England). All other reagents were of analytical grade.

Purification of Tubulin. Goat brain microtubule protein was isolated by two cycles of polymerization and depolymerization in the presence of 1 M sodium glutamate and 10% (v/v) dimethyl sulfoxide (*36*). Bovine microtubule protein was purified as previously described (*37*). The tubulin was purified from the microtubule protein preparations by phosphocellulose chromatography and stored at −80 °C. The tubulin concentration throughout this paper was determined by the method of Bradford using bovine serum albumin (BSA) as a standard (*38*).

Spectral Measurements. All fluorescence measurements were performed using a JASCO FP-6500 spectrofluorometer equipped with a constant-temperature water-circulating bath. Spectra were taken by multiple scans, and buffer blank values were subtracted from all measurements. A 0.3-cm path-length cuvette was used for all fluorescence measurements that minimized the inner-filter effects at high benomyl concentrations. All absorbance measurements were performed in a JASCO V-530 UV−visible spectrophotometer using a 1-cm path-length cuvette. The far-UV (215−250 nm) circular dichroism (CD) spectra were recorded at 25 °C using a JASCO spectropolarimeter (model J-810) equipped with a JASCO PTC 423S Peltier temperature-control system. A quartz cuvette of 1-mm path length was used for the far-UV CD measurements. Spectra were collected with a scan speed of 200 nm/min and a response time of 1 s. Each spectrum was the average of three scans. The CD data were analyzed using JASCO.

Inhibition of Purified Tubulin Assembly by Benomyl. Goat brain tubulin (1.2 mg/mL) was mixed with different concentrations of benomyl at 0 °C (0−120 μM) in an assembly buffer (25 mM pipes at pH 6.8, 3 mM $MgS0_4$, 1 mM EGTA, 1 mM GTP, and 1 M sodium glutamate). Polymerization was initiated by raising the temperature to 37 °C in the water bath. The rate and extent of the polymerization reaction were monitored by light scattering at 350 nm (*39*). For the sedimentation assay, tubulin (1.2 mg/mL) was polymerized in an assembly buffer in the absence and presence of different concentrations of benomyl for 45 min at 37 °C. The polymers were collected by sedimentation at 50000*g* for 45 min at 30 °C.

Electron Microscopy. Tubulin (1.2 mg/mL) was polymerized in the absence and presence of 50 and 100 μM benomyl as described in the previous paragraph. The

[1] Abbreviations: pipes, 1,4-piperazinediethanesulfonic acid; MES, 2-(*N*-morpholino)ethanesulfonic acid; EGTA, [ethylenebis (oxyethylenenitrilo)]tetraacetic acid; GTP, guanosine-5′-triphosphate; ANS, 1-anilinonaphthalene-8-sulfonic acid; DTNB, 5,5′-dithiobis-2-nitrobenzoic acid; DAPI, 4′,6-diamidino-2-phenylindole.

polymers were fixed with prewarmed 0.5% glutaraldehyde for 5 min. Samples (20 μL) were applied to carbon-coated electron microscope grids (300 mesh) for 30 s and blotted dry. The grids were subsequently negatively stained with a 1% uranyl acetate solution and air-dried. The samples were viewed in a Philips CM 200 electron microscope. Images were taken at 13 500 × and 35 000 × magnifications (*37*).

Binding Measurements. Binding of benomyl to goat brain tubulin was determined by using hydrophobic fluorescent probe 1-anilinonaphthalene-8-sulfonic acid (ANS). We took advantage of the finding that benomyl increases the fluorescence of tubulin-bound ANS (*40*). Tubulin (1 μM) was first incubated with different concentrations (1−50 μM) of benomyl in 25 mM pipes at pH 6.8, 3 mM $MgS0_4$, and 1 mM EGTA at 25 °C for 30 min. ANS (40 μM) was then added to the reaction mixtures and incubated for an additional 15 min. The excitation and emission wavelengths were 400 and 470 nm respectively. Benomyl has negligible absorption at 470 nm. The extinction coefficients of benomyl at 360 and 400 nm were determined to be 2018 and 1574 M^{-1} cm^{-1}, respectively. Corrections because of the inner-filter effects were made according to the formula $F = F_{obs}$ antilog $[(A_{ex} + A_{em})/2]$, where A_{ex} is the absorbance of benomyl at the excitation wavelength and A_{em} is the absorbance at the emission wavelength (*41*). The fraction of the binding sites (X) occupied by benomyl was determined using the equation $X = (F - F_o)/F_{max}$, where F_o is the fluorescence intensity of tubulin−ANS in the absence of benomyl, F is the corrected fluorescence intensity of tubulin−ANS in the presence of benomyl, and F_{max} was calculated from the plot of $1/(F - F_o)$ versus 1/[benomyl] and extrapolating 1/[benomyl] to zero. The dissociation constant (K_d) was determined using the relationship, $1/X = 1 + K_d/L_f$, where L_f represents the free benomyl concentration, and $L_f = C - X[Y]$, where C is total concentration of benomyl and $[Y]$ is the molar concentration of ligand-binding sites assuming a single binding site per tubulin dimer (*42*).

Colchicine Binding to Tubulin. Colchicine binding to goat tubulin was determined by using the increase in the intrinsic fluorescence of colchicine upon the binding of colchicine to tubulin (*43*). The excitation and emission wavelengths were 360 and 430 nm, respectively.

Titration of Tubulin Sulfhydryl Groups. The sulfhydryl-specific reagent 5,5′-dithiobis-2-nitrobenzoic acid (DTNB) complexes with thiol groups in tubulin, and the rate and extent of sulfhydryl-group modification can be monitored by measuring the absorbance change at 412 nm (*44*). Tubulin (3 μM) was incubated with 50 μM benomyl at 4 °C for 15 min, and then 100 μM DTNB was added. The number of sulfhydryl groups modified after 30 min of reaction was determined by using a molar extinction coefficient of 12 000 for DTNB at 412 nm.

Effects of Benomyl on Microtubule Dynamics. Microtubule dynamics were measured by video microscopy by the procedure of Panda et al. (*45*) as modified by C. Newton (University of California, Santa Barbara, to be published). Flow-cell chambers of approximately 10 μL of volume were constructed using two pieces of double-stick tape, a glass slide, and a coverslip. Sea urchin (*Strongylocentrotus purpuratus*) axonemes used to seed microtubule polymerization were flowed through the chamber, and the chamber was incubated at 30 °C to allow the axonemes to stick to the glass surface. The chambers were then washed with a buffer containing 87 mM pipes, 36 mM MES, 1.4 mM $MgCl_2$, 1 mM EGTA, and 1 mM GTP at pH 6.8 (PMME), and a sample containing 19 or 22 μM bovine brain tubulin in 1 mM GTP was then flowed through the chamber by wicking the opposite end with small pieces of Whatman filter paper. The chamber was sealed at both ends with drops of VALAP (vasoline/lanolin/paraffin, 1:1:1). The microtubules were then assembled onto the axoneme seeds by placing the slide onto a prewarmed (30 °C) microscope stage and allowing the slide to incubate for 30 min to achieve a steady state. The dynamic-instability behavior of the microtubules was imaged by video-enhanced differential interference contrast microscopy using a Zeiss IM35 inverted microscope with a 63× (1.4 na) oil-immersion objective. Growth of the microtubules occurred at both the plus and minus ends of the axonemes. The plus ends of the microtubules were distinguished from the minus ends by their higher growth rates, greater excursion lengths, and larger number of microtubules per axoneme end as previously reported (*37*, *45*). Samples on the slides were recorded for a maximum of 60 min, and individual microtubules were recorded and analyzed between 2 and 10 min. Microtubule lengths were measured and analyzed as previously described (Panda et al., 2003). Growth and shortening events were determined by least-squares regression of the life-history plots of microtubule length versus time. The dynamic instability parameters were determined as previously described (*46*).

Cell Culture and Proliferation Assay. HeLa cells were grown in minimal essential medium (Himedia) supplemented with 10% (v/v) fetal bovine serum, kanamycin (0.1 mg/mL), penicillin G (100 units/mL), and sodium bicarbonate (30 mg/mL) at 37 °C in 5% CO_2. Cell proliferation was determined in 96-well plates using the sulforhodamine B assay as previously described (*47*). In brief, 1×10^4 cells were seeded in each well. Approximately 24 h later, cells were incubated with different concentrations of benomyl for an additional 24 h. Cells were then fixed with 10% trichloroacetic acid and stained with 0.4% sulforhodamine B dissolved in 1% acetic acid. Each assay condition within an experiment was carried out three times, and three replicate experiments were performed.

Immunofluorescence Microscopy. Immunofluorescence microscopy was performed as previously described with slight modification (*48*). Cells were grown on coverslips at a density of 1×10^5 cells/mL in 24-well plates. Cells were fixed in 3.7% formaldehyde for 30 min at 37 °C and then transferred to cold (−20 °C) methanol for 10 min. Nonspecific antibody binding sites were blocked by incubating with 2% BSA in phosphate-buffered saline (PBS) at 37 °C for 15 min. Cells were then incubated for 2 h at 37 °C with a mouse monoclonal antitubulin antibody (1:150 dilution in 2% BSA/PBS). Cells were then washed with 2% BSA/PBS for 10 min at room temperature before incubating with a 1:100 dilution of an Alexa-568-labeled anti-mouse IgG antibody (Molecular Probes) at 37 °C for 1 h. Coverslips were then rinsed with 2% BSA/PBS for 10 min and incubated with DAPI (1 μg/mL) for 30 s at room temperature. The coverslips were mounted in 50% glycerol in PBS containing 1 mg/mL ascorbic acid. The microtubules (red) and chromosomes (blue) were observed with a Nikon Eclipse TE-

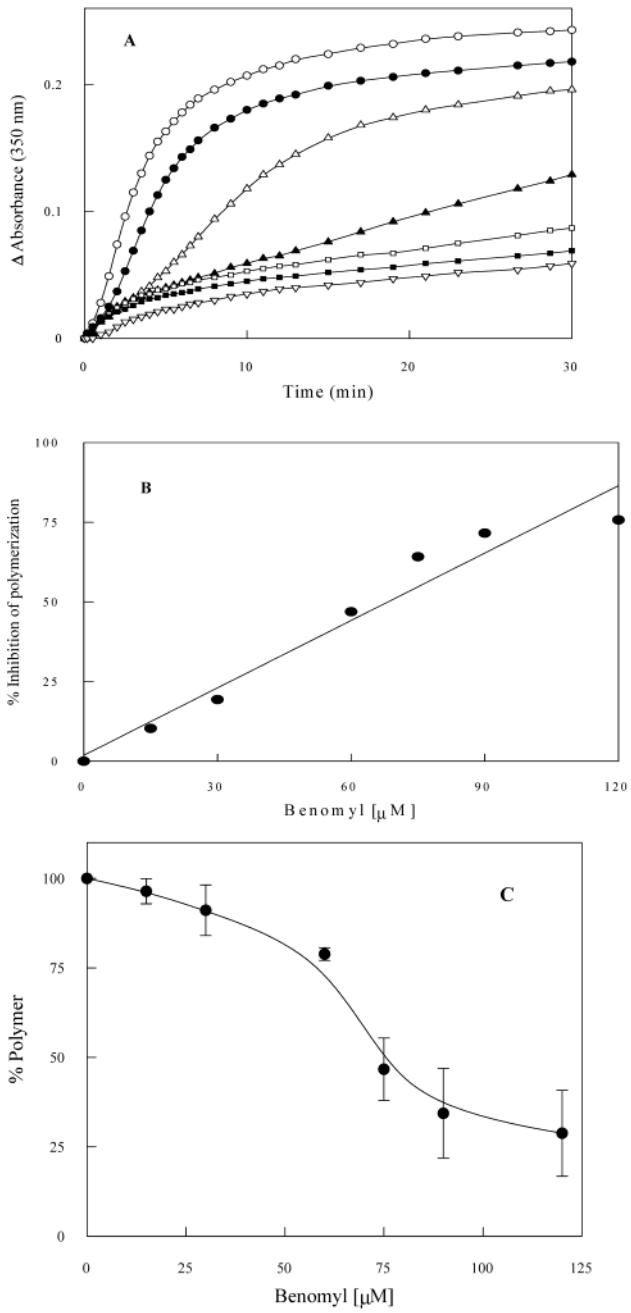

FIGURE 2: Inhibition of microtubule assembly by benomyl. (A) Polymerization of tubulin (12 μM) in the assembly buffer was measured in the absence (○) and presence of 15 (●), 30 (△), 60 (▲), 75 (□), 90 (■), or 120 μM (▽) benomyl. Microtubule assembly was monitored by measuring the increase in the absorbance values at 350 nm with time. (B) Inhibition of tubulin polymerization at 30 min is plotted as a function of the benomyl concentration. (C) Effects of benomyl on the microtubule polymer mass. Tubulin (12 μM) was polymerized in an assembly buffer at 37 °C for 45 min in the absence or presence of different benomyl concentrations. The microtubule polymer mass was determined as described in the Experimental Procedures. Data are the average of four independent experiments.

2000U microscope. The images were analyzed using Image-Pro.

Mitotic Indices. Mitotic indices were determined by staining HeLa cells with Wright−Giemsa (*49*). Briefly, cells were plated at a density of 1.0×10^4 cells in 24-well plates 24 h prior to the addition of benomyl. They were treated with different concentrations of benomyl for an additional 24 h. Both attached and unattached cells were harvested by trypsinization, washed with PBS, and then treated with 0.5% KCl for 10 min at room temperature. After centrifugation, the cells were fixed with a methanol/acetic acid solution (3:1, v/v). Finally, the cell suspensions were spread onto cold slides, air-dried, and stained with a 10% Giemsa solution. At least 200 cells were counted at each benomyl concentration. The mitotic index was determined as described previously (*49*).

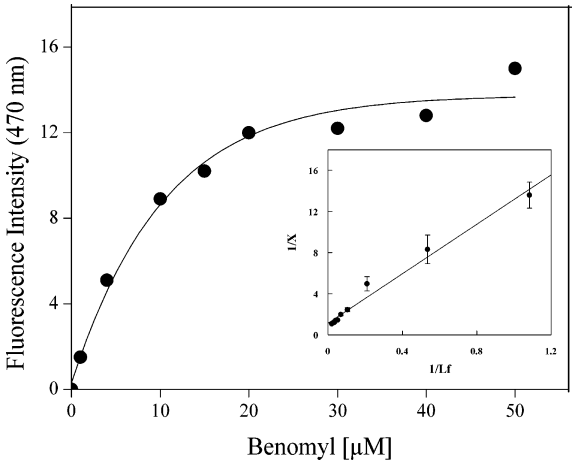

FIGURE 3: Determination of binding parameters of benomyl to tubulin by the tubulin−ANS complex fluorescence. The figure shows the titration of 1.0 μM tubulin, preincubated with different concentrations (1−50 μM) of benomyl at 25 °C for 30 min, with 40 μM of ANS. Spectra were taken after an incubation for 15 min at 25 °C. The excitation and emission wavelengths were 400 and 470 nm, respectively. The inset shows a double reciprocal plot of the binding of benomyl to tubulin. Data are an average of 9 independent experiments. Error bars are the standard error of the mean.

RESULTS

Inhibition of Tubulin Polymerization by Benomyl. We determined the effects of benomyl on the polymerization of purified goat brain tubulin into microtubules by two complementary techniques, light scattering and sedimentation. Purified goat brain tubulin (12 μM) was polymerized in the absence or presence of different concentrations of benomyl. As shown in Figure 2A, benomyl produced a concentration-dependent inhibition of the rate and extent of microtubule polymerization. A concentration of 30 μM benomyl decreased the extent of polymerization at 30 min by ~20%, while 120 μM benomyl inhibited polymerization by ~75% at the same time. Half-maximal inhibition (IC_{50}) of polymerization was calculated to be 69 ± 10 μM (Figure 2B). The ability of benomyl to inhibit microtubule polymerization was also determined by a sedimentation assay. Benomyl also inhibited polymerization in this assay in a concentration-dependent fashion (Figure 2C) with half-maximal inhibition of polymerization occurring at 75 ± 5.5 μM benomyl. Electron microscopic analysis showed that microtubules in the absence and presence of 50 and 100 μM benomyl had similar morphology (data not shown).

Affinity of Benomyl Binding to Tubulin. The tryptophan residues in tubulin are intrinsically fluorescent, and modulation of tryptophan fluorescence by ligands as determined by fluorescence spectroscopy has been used extensively to

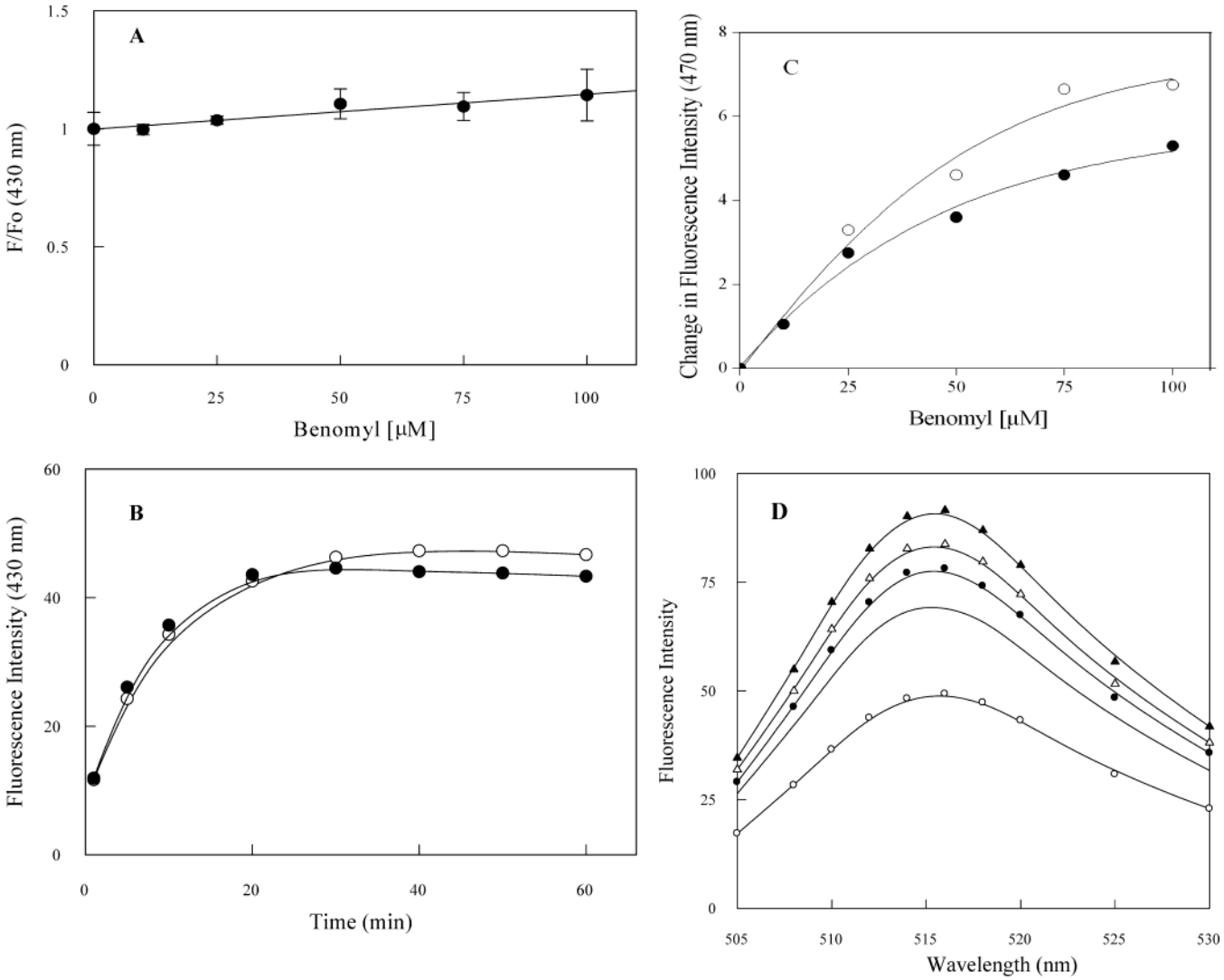

FIGURE 4: Inhibition of colchicine binding to tubulin by benomyl. (A) Tubulin (5.0 μM) was first incubated with different concentrations of benomyl at 37 °C for 30 min, and then 10 μM colchicine was added to each of the mixtures. Fluorescence was measured after an incubation for 60 min at 37 °C. The excitation and emission wavelengths were 360 and 430 nm, respectively. Data are the average of four independent experiments. (B) Kinetics of colchicine binding to tubulin. The binding of colchicine to tubulin at 37 °C was determined in the absence (○) and presence (●) of 100 μM benomyl by exciting the samples at 360 nm. (C) Effects of benomyl on the tubulin−ANS complex fluorescence in the absence (○) and presence (●) of colchicine. The tubulin−colchicine complex was prepared as described in A by using 3.0 μM tubulin and 20 μM colchicine, and a fixed concentration (50 μM) of ANS was added. Different concentrations of benomyl (0−100 μM) were then added, and fluorescence was determined after an incubation for 30 min at 25 °C. The excitation and emission wavelengths were 400 and 470 nm, respectively. (D) Competition between benomyl and vinblastine. Tubulin (3.0 μM) was first incubated with the vehicle, DMSO (−), 200 μM vinblastine (○), and 25 (●), 50 (△), and 100 μM (▲) benomyl at 37 °C for 45 min, and then 2 μM BODIPY FL-vinblastine was added to all of the mixtures. Fluorescence was measured after an incubation for 20 min at 25 °C. The excitation wavelength was 490 nm. The bound fluorescence spectra of the tubulin−BODIPY FL-vinblastine complex were obtained by subtracting the fluorescence spectra of unliganded BODIPY FL-vinblastine in the absence of tubulin (blank spectra) from the spectra of BODIPY FL-vinblastine in the presence of tubulin.

investigate the binding of ligands to tubulin. However, like tubulin, benomyl absorbs at 295 nm and fluoresces at 335 nm, and we could not detect a quantifiable change of tubulin fluorescence intensity at 335 nm upon binding of benomyl using this approach (data not shown). Hydrophobic fluorescent probes are also routinely used to monitor ligand binding to tubulin. We found that we could use fluorescent probe ANS to investigate the binding of benomyl to tubulin (*40*). The effects of different concentrations of benomyl on the fluorescence of tubulin−ANS complexes are shown in Figure 3. Benomyl increased the fluorescence of the complex in a concentration-dependent manner. The inset in Figure 3 shows a double reciprocal plot of the binding data. The linear regression of the data, assuming a single binding site for benomyl per tubulin dimer, yielded a dissociation constant (K_d) of 11.9 ± 1.2 μM.

Location of the Benomyl-Binding Site in Tubulin. Colchicine and vinblastine are well-characterized drugs that bind to tubulin, inhibit microtubule polymerization, and suppress microtubule dynamic instability (*25*−*28*). Despite their similar actions, the colchicine- and vinblastine-binding sites in tubulin are different. Considerable evidence indicates that several benzimidazoles share their binding site on tubulin with colchicine (*5*−*7*). However, recently, Downing and coworkers have suggested that benomyl binds to tubulin at a site that is different from the colchicine site (*9*−*11*). Therefore, we wanted to determine whether benomyl could compete with colchicine for binding to tubulin. Colchicine

is weakly fluorescent in an aqueous solution but becomes strongly fluorescent when it binds to tubulin (*43*). Thus, we used the fact that the tubulin−colchicine complex fluoresces to determine whether benomyl could compete with colchicine binding to tubulin. First, we found that preincubation of tubulin with benomyl (10−100 μM) did not affect the binding of colchicine to tubulin as determined by colchicine fluorescence (Figure 4A). These data indeed suggest that benomyl does not bind to the colchicine site. In addition, we found that, when benomyl (10−100 μM) was incubated with the preformed tubulin−colchicine complex for 30 min, it did not decrease the fluorescence of the complex. Specifically, incubation of the preformed tubulin−colchicine complex with 50 or 100 μM benomyl did not decrease, and actually slightly increased, the fluorescence signal of the preformed tubulin−colchicine complex (by 8 and 12%, respectively). We also measured the kinetics of colchicine binding to tubulin in the absence and presence of benomyl. Preincubation of 100 μM benomyl with tubulin did not reduce the rate of colchicine binding to tubulin (Figure 4B), which further supports the conclusion that benomyl does not bind to the colchicine site.

In further analysis of this question, we used ANS fluorescence as a probe to determine whether benomyl binds at the colchicine-binding site. ANS binds to tubulin at a site that is distinct from the colchicine-binding site, and it is known that colchicine binding to tubulin does not interfere with ANS binding to tubulin (*40*). First, the tubulin−colchicine complex was formed by incubating tubulin (3 μM) with 20 μM colchicine at 37 °C for 60 min. Then, ANS (50 μM) was added to the tubulin−colchicine complex. Figure 4C shows that incubation of the ANS−tubulin or ANS−tubulin−colchicine complex with benomyl increased the fluorescence both of the ANS−tubulin and ANS−tubulin−colchicine complex in a benomyl-concentration-dependent manner. The increase in bound ANS fluorescence with an increasing benomyl concentration was found to be similar both for tubulin and the tubulin−colchicine complex suggesting that benomyl and colchicine can bind to tubulin simultaneously. When taken together, the experiments strongly support the conclusion that benomyl and colchicine bind to different sites on tubulin. We also measured the possible competition between benomyl and vinblastine for the vinblastine-binding site in tubulin by using a fluorescent analogue of vinblastine (BODIPY FL-vinblastine). Addition of benomyl increased the fluorescence of the BODIPY FL-vinblastine (Figure 4D) indicating that benomyl also does not bind to the vinblastine site in tubulin. The increase in fluorescence of the tubulin−BODIPY FL-vinblastine complex in the presence of a high concentration of benomyl was likely due to a stabilization of the vinblastine-binding site of tubulin by benomyl. Ligand-induced stabilization of the vinblastine, colchicine, and GTP sites has been known for years (*32*, *50*).

Evidence that the Binding of Benomyl to Tubulin Induces a Conformational Change in the Tubulin. The sulfhydryl groups of tubulin are sensitive markers for studying tubulin conformation and for its interaction with ligands (*51*−*53*). We used the sulfhydryl-specific reagent DTNB to determine the accessibility of the cysteine residues of tubulin toward modification in association with benomyl binding. The reaction kinetics for cysteine titration in tubulin with DTNB at 37 °C in the absence and presence of 50 μM benomyl are shown in Figure 5. Benomyl significantly reduced the number of cysteine residues accessible to DTNB; there were 11.5 ± 0.2 sulfhydryl residues accessible per tubulin dimer in the absence of benomyl and 9.2 ± 0.4 residues per tubulin dimer in the presence 50 μM benomyl. The difference in the number of modified cysteine residues in the absence and presence of 50 μM benomyl was 2.3 ($P < 0.01$, Student's two-tailed t test). These data indicate that the binding of benomyl to tubulin induces a conformational change in the tubulin. Changes in the CD spectra indicated that binding of benomyl to tubulin can also affect the secondary structure of tubulin. As shown in Figure 6, both 25 and 50 μM benomyl altered the amplitude of the far-UV tubulin spectrum, indicative of a change in the secondary structure of tubulin.

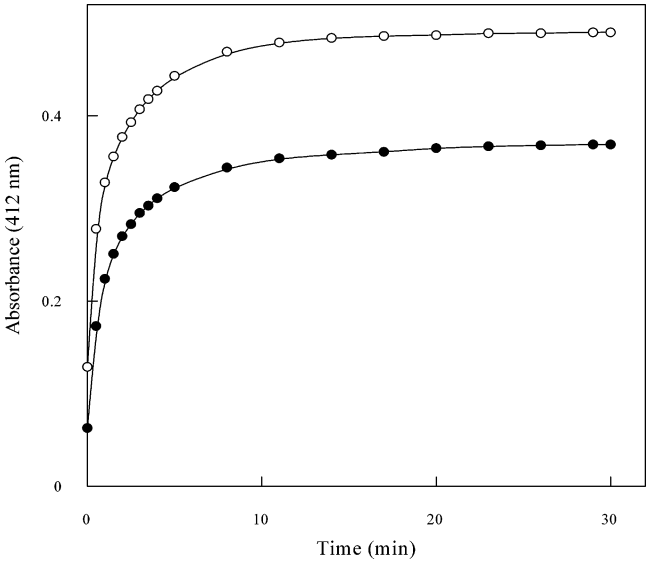

FIGURE 5: Reduction of sulfhydryl group accessibility by benomyl. The rate and extent of sulfhydryl group modification were monitored by measuring the absorbance at 412 nm. Tubulin (3 μM) was incubated in the absence (○) or presence (●) of 50 μM benomyl at 4 °C for 15 min, and then 100 μM DTNB was added. After incubation for 30 min at 37 °C, the number of sulfhydryl groups modified in the absence and presence of 50 μM benomyl were determined from 12 independent measurements as described in the Experimental Procedures.

Effects of Benomyl on the Dynamics of Individual Microtubules in Vitro. We then analyzed the effects of benomyl on the dynamic instability at the plus ends of individual bovine brain microtubules at steady-state in vitro video microscopy. The quantitative effects of benomyl on the individual dynamic parameters are shown in Table 1. Benomyl reduced the growing rate, shortening rate, and dynamicity, in a concentration-dependent manner. Specifically, 30 μM benomyl reduced the growing rate, shortening rate, and dynamicity of the microtubules by 49, 49, and 65%, respectively. Benomyl did not affect the catastrophe or rescue frequencies.

Inhibition of Mammalian Cell Proliferation and Mitosis by Benomyl. Benomyl inhibits cell proliferation and mitosis by an action on microtubules in sensitive fungal cells, but little is known about the antiproliferative and antimitotic activities of benomyl in mammalian cells. It is considered

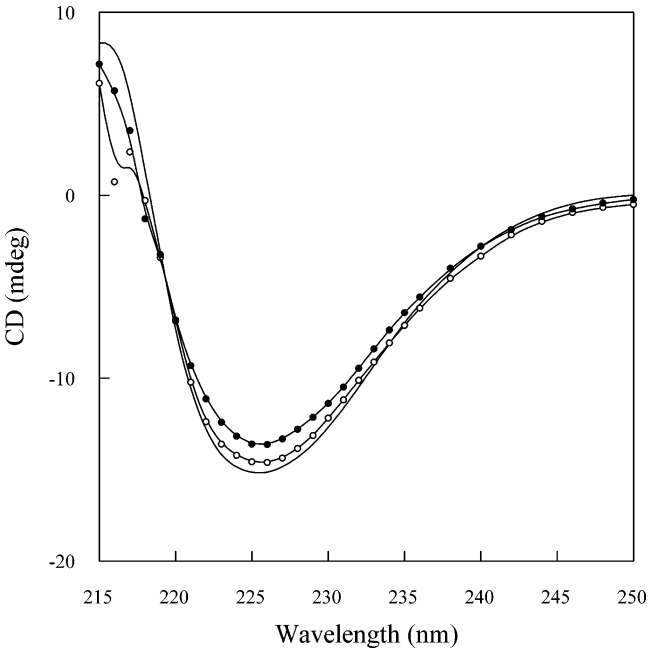

FIGURE 6: Effect of benomyl on the CD spectrum of tubulin. The graph shows the far-UV CD spectra of 3 μM tubulin in the absence (—) and presence of 25 (○) and 50 μM (●) benomyl in a 10 mM phosphate buffer (pH 6.8). Tubulin (3 μM) was incubated in the absence and presence of benomyl at 25 °C for 30 min, and the far-UV spectra were collected using a quartz cuvette of 1-mm path length as described in the Experimental Procedures. Each spectrum was the average of three scans. One of the four similar experiments is shown in the figure.

to have little if any effect on mammalian cells. Thus, it was surprising that benomyl suppressed the dynamics of bovine brain microtubules so effectively. To determine the extent to which benomyl inhibits mitosis in mammalian cells, we investigated the ability of benomyl to inhibit proliferation of a human tumor (HeLa) cell and determined its effects on mitosis and mitotic spindle organization. We found that benomyl caused a concentration-dependent inhibition of HeLa cell proliferation with IC_{50} of 5 ± 1 μM (Figure 7A). We also found that it inhibited the cell-cycle progression during mitosis, with a reasonably similar IC_{50} of ~15 μM (Figure 7B).

Cells were also treated with benomyl or with the vehicle alone (DMSO) for 24 h and processed to immunofluorescence microscopy to analyze the effects of the compound on the organization of the spindle microtubules and chromosomes in the blocked cells. Untreated cells at metaphase of mitosis displayed normal spindle microtubule morphology, and the mitotic chromosomes were well-aligned at the metaphase plate (parts A and B of Figure 8). The spindle microtubules in the cells treated with 5 μM benomyl appeared nearly normal, but some of the chromosomes were unable to congress to the metaphase plate (parts C and D of Figure 8). Cells treated with four times the IC_{50} concentration for inhibition of proliferation (parts E and F of Figure 8) had clear abnormalities typical to those observed with relatively high concentrations of drugs such as vinblastine (*48*, *54*). Also typical of the more potent antimitotic drugs, benomyl did not appear to significantly disrupt the organization or depolymerize the microtubules in interphase cells at concentrations at which it caused inhibition of mitosis (Figure 9).

DISCUSSION

Benomyl is a widely used antimitotic antifungal compound both in agriculture and as a research tool in the biology of fungal-cell systems (*1*−*3*). It is selectively toxic to fungal-cell tubulin and appears to have relatively low toxicity in mammalian systems (*1*, *4*−*8*). It has been thought, though little data exist, that it has low toxicity in humans because it has very low affinity for mammalian tubulin (*4*, *7*). In this paper, we investigated the interaction of benomyl with mammalian brain tubulin and microtubules and found that the compound binds to mammalian tubulin with a K_d of 11.9 ± 1.2 μM, somewhat stronger than what had been thought. On the basis of the fact that benomyl is a benzimidazole, it was also thought that benomyl might bind to the colchicine-binding site in β tubulin. However, evidence involving site-directed mutagenesis in yeast cells (*9*−*19*) and direct biochemical data described here strongly suggest that the benomyl-binding site is distinct from the colchicine site.

We found that benomyl inhibits the polymerization of brain tubulin, with 50% inhibition (IC_{50}) of polymerization occurring at a benomyl concentration of 70−75 μM. Thus, its ability to inhibit microtubule polymerization is not especially robust. However, we found that benomyl suppresses the dynamic instability behavior of the microtubules fairly strongly. On the basis of the stronger than expected effects of benomyl on tubulin and microtubules in vitro, we also examined the effects of benomyl on HeLa cell proliferation and mitosis and found, surprisingly, that benomyl inhibits proliferation of the cells with an IC_{50} of 5 μM and that it blocks the mitotic spindle function by perturbing the microtubule and chromosome organization. These actions on mammalian-cell tubulin and microtubules suggest that the toxicity of benomyl in humans may be due in part to the perturbation of microtubule function.

Benomyl Binds to Mammalian Brain Tubulin with Moderate Affinity at a Site Distinct from the Colchicine-Binding Site. We used fluorescent probe ANS to determine the binding affinity of benomyl for mammalian brain tubulin. Using ANS, we obtained a K_d of 11.9 ± 1.2 μM. Thus, the affinity of benomyl for brain tubulin is not robust, but a K_d in the 10 μM range indicates that benomyl binds to mammalian brain tubulin with moderate affinity rather than weak affinity. Colchicine binds to tubulin with high affinity (K_d ~ 0.1−0.5 μM) (*28*, *30*).

Previously, it was shown that a number of benzimidazole analogues inhibit the binding of colchicine both competitively and noncompetitively (*4*−*6*). On the basis of the structural similarities between benomyl and other benzimidazoles, it was thought that all benzimidazole analogues would bind near or at the colchicine site. However, to our knowledge, no direct analyses have been done to determine whether benomyl in fact binds to, at, or near the colchicine-binding site. Recently, using site-directed mutagenesis of yeast tubulin coupled with structural analysis, Downing et al. (*9*−*11*) proposed that the benomyl site is located in a central region of β tubulin at a site distinct from the colchicine site because the colchicine site is considered to be located at the interface between α and β tubulin. In the present paper, we found that benomyl does not interfere with colchicine binding to tubulin and that benomyl and colchicine can bind simultaneously to tubulin. Thus, our data are consistent with

Table 1: Comparison of Steady-State in Vitro Microtubule Dynamics at the Plus Ends in the Presence of Benomyl

parameter	control	5 μM	15 μM	30 μM
		Mean Rates[a] (μm/min)		
growth	1.00 ± 0.78	0.78 ± 0.39	0.87 ± 0.61	0.51 ± 0.35[b]
shortening	18.37 ± 13.23	18.05 ± 12.18	10.88 ± 9.57[b]	8.96 ± 7.62[c]
		Mean Duration (min)		
growth	1.69 ± 1.62	2.04 ± 1.42	1.61 ± 1.00	2.75 ± 1.36[c]
shortening	0.35 ± 0.27	0.33 ± 0.17	0.51 ± 0.21	0.40 ± 0.24
attenuation	1.21 ± 1.39	1.66 ± 1.74	1.75 ± 1.12	2.62 ± 2.10[c]
		% Time Spent		
growth	63.2	63.4	64.5	51.6
shortening	13.8	10.9	10.4	9.7
attenuation	23.0	25.8	25.1	38.7
		Frequency of (min^{-1})		
catastrophe	0.43 ± 0.06	0.37 ± 0.06	0.26 ± 0.06	0.30 ± 0.07
rescue	1.42 ± 0.26	1.75 ± 0.37	1.98 ± 0.44	2.08 ± 0.54
dynamicity (μm/min)	3.17	2.46	1.69	1.13
minutes	158	115	97	75

[a] Standard deviation values are shown. [b] Statistically significant, at the 95% level, to the corresponding control value. [c] Statistically significant, at the 99% level, to the corresponding control value.

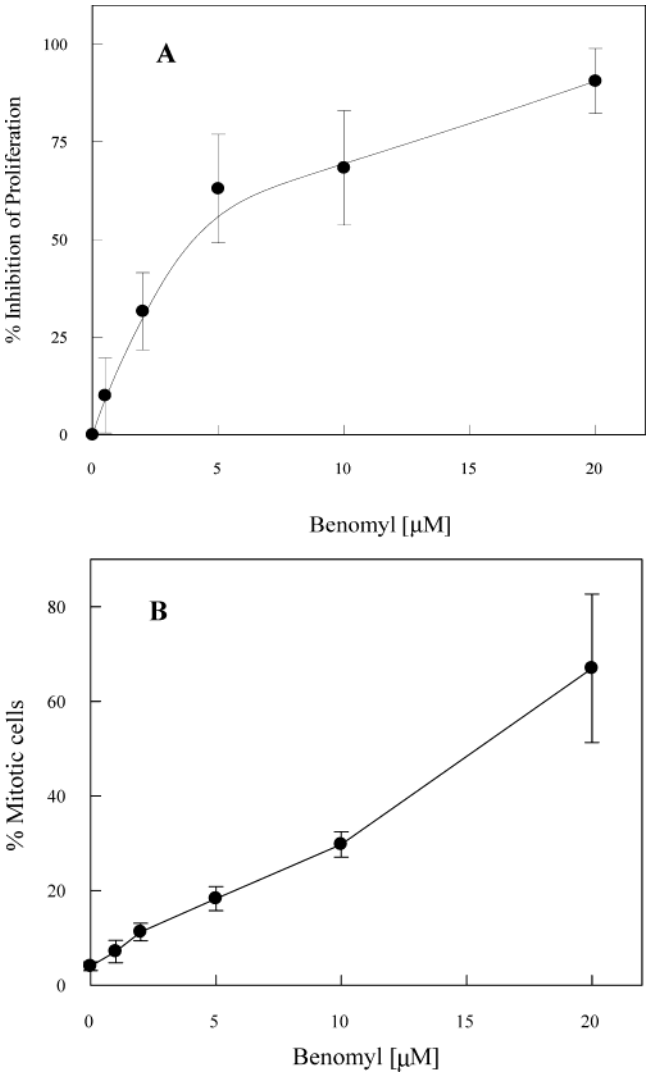

FIGURE 7: Effect of benomyl on HeLa cell proliferation (A) and the mitotic index (B). The inhibition of cell proliferation and the mitotic index was determined by sulforhodamine B assay and Wright−Giemsa staining, respectively, as described in the Experimental Procedures.

the conclusions of Richards et al. (*11*) and Downing (*9*, *10*), on the basis of site-directed mutagenesis of the β-tubulin gene in the yeast *S. cerevisiae*, that the benomyl site is located in the core of β tubulin and the colchicine-binding site is located in the interface between α and β tubulin as proposed.

Effects of Benomyl on the Conformation of Tubulin. The binding of benomyl to brain tubulin increased the fluorescence of tubulin-bound ANS and affected the accessibility of the sulfhydryl groups of tubulin to DTNB, indicating that benomyl binding to the tubulin induced a conformational change in the tubulin. The binding of benomyl to brain tubulin also induced changes in the far-UV CD spectrum of the tubulin, indicating that benomyl induces conformational change in its secondary structure. When taken together, the results indicate that the binding of benomyl to brain tubulin modifies the conformation of the tubulin in some way.

Mechanism of Inhibition of Microtubule Polymerization and Dynamics by Benomyl. While benomyl is believed to have minimal toxic effects in vertebrates (*4*), previous studies (*5*, *55*) and the results reported here show that benomyl can weakly inhibit mammalian microtubule polymerization. Specifically, we found that benomyl inhibited the polymerization of goat brain tubulin into microtubules with an IC_{50} of ~70 μM (Figure 2). We also found that benomyl suppressed the dynamic instability behavior of bovine brain microtubules with greater than expected potency. Its main effects were to reduce the growing and shortening rates of the microtubules, which resulted in a reduced overall dynamicity (Table 1). Interestingly, benomyl did not alter the switching frequencies, i.e., the catastrophe and rescue frequencies, which are thought to be related to the loss and gain of the stabilizing "GTP cap" at the microtubule ends. Therefore, it may be that benomyl does not act or bind at the microtubule ends such as colchicine or vinblastine, both of which do affect the transition frequencies (*25*−*28*).

Interestingly, high concentrations of benomyl were required to inhibit microtubule polymerization (IC_{50} ~ 70 μM), whereas its affinity (K_d) for tubulin was 11.9 ± 1.2 μM. One can calculate that, at the benomyl concentration that caused half-maximal inhibition of polymerization, most (nearly 85%) of the soluble tubulin should be complexed with benomyl. Therefore, benomyl probably does not inhibit microtubule polymerization through a simple end-poisoning

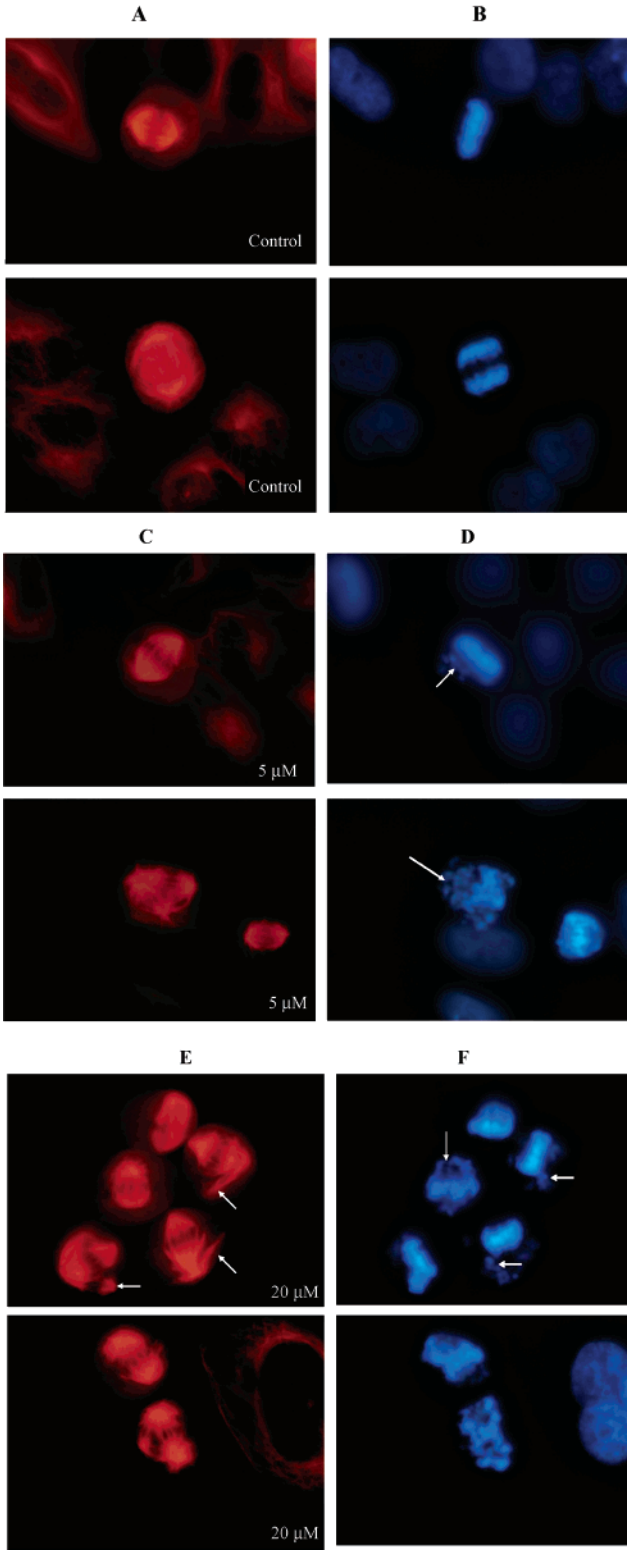

FIGURE 8: Effects of benomyl on spindle microtubule and chromosome organizations of the HeLa cells. HeLa cells were grown in the absence and presence of 5 and 20 μM benomyl for 24 h. Microtubules are shown in A (control), C (5 μM benomyl), and E (20 μM benomyl), and chromosome organizations of the corresponding cells are shown in B, D, and F. A control mitotic HeLa cell with a well-defined compact metaphase plate of chromosomes is shown in the upper parts of A and B. The lower parts of A and B showed a normal HeLa cell in anaphase. Mitotic cells treated with 5 μM benomyl (C and D) showed abnormal bipolar spindle with one uncongressed chromosome at one spindle pole (arrow). Another cell had tripolar spindle organization (bottom parts of C and D).

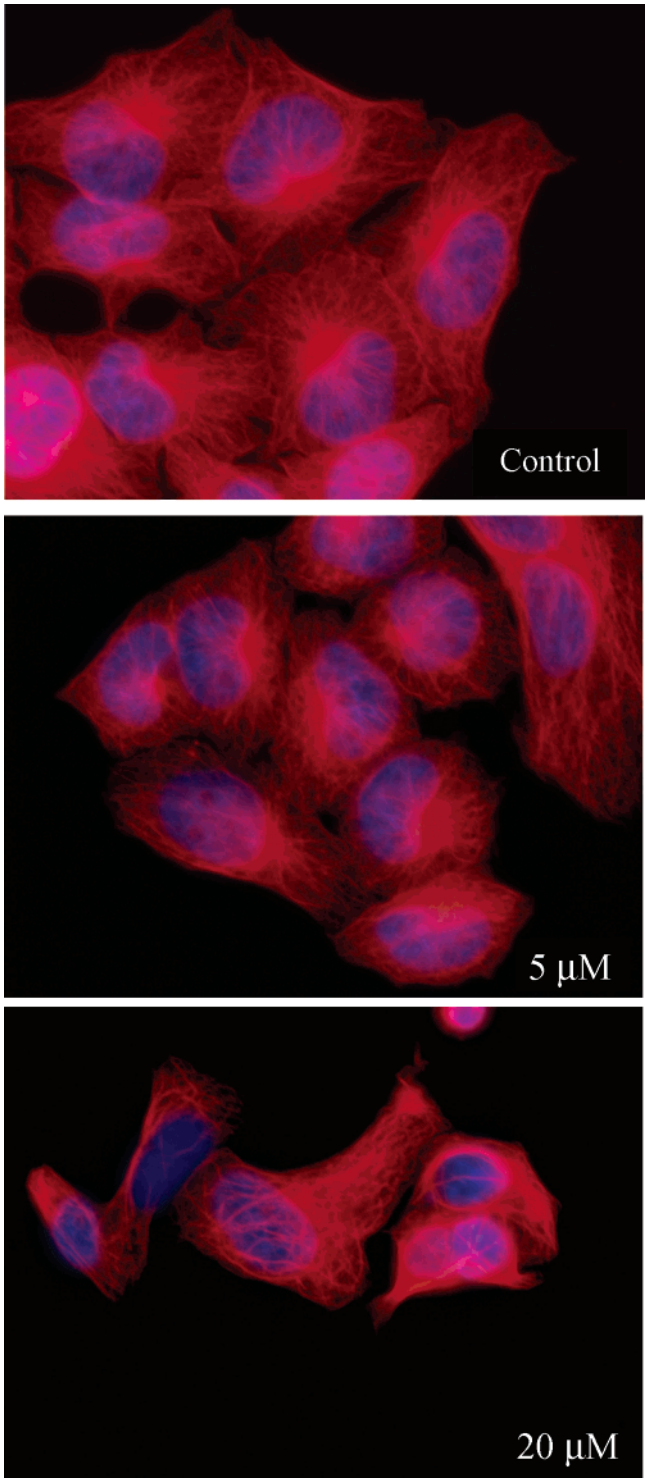

FIGURE 9: Effects of 5 and 20 μM benomyl on interphase microtubules in HeLa cells exposed for 24 h.

mechanism, which occurs with colchicine and vinblastine (*56*−*59*). More likely, benomyl as a benomyl−tubulin complex copolymerizes along with free tubulin into microtubules. If so, the incorporation of large numbers of the benomyl−tubulin complexes in the polymer only weakly inhibits polymerization. In further support of the hypothesis that benomyl copolymerized with tubulin into the microtubules, benomyl especially suppressed the shortening rate. Thus, benomyl must be present in the microtubule itself to be able to inhibit the rate of shortening if it is not acting directly at the microtubule ends.

Benomyl induced conformational changes in tubulin (Figures 5 and 6), and it is possible that the deformation induced by benomyl in the tubulin structure, while permitting the tubulin to incorporate into the microtubule, prevented proper addition of the tubulin such that the growing rate was reduced. Similarly, the presence of benomyl in the polymer could stabilize the lattice, thereby reducing the shortening rate. The colchicine−tubulin complex also copolymerizes with free tubulin into microtubules, but the degree of copolymerization with colchicine is clearly low as compared with the degree of copolymerization that appears to occur with benomyl (*45*, *56*−*58*). It is tempting to suggest that the ability of the benomyl−tubulin complexes to copolymerize efficiently with tubulin into mammalian microtubules, which produces relatively small effects on the polymer mass, contributes to its low toxicity against mammalian cells.

Inhibition of HeLa Cell Proliferation and Mitosis. A number of previous reports have shown that benomyl strongly inhibits cell proliferation at mitosis in fungal cells (*4*, *7*). Here, we found that benomyl also inhibits cell proliferation at mitosis in a mammalian (HeLa) cell, albeit more weakly that in fungal cells. Specifically, benomyl inhibited HeLa cell proliferation with an IC_{50} of ~5 μM (Figure 7A) and caused the accumulation of cells at prometaphase and metaphase of mitosis with an IC_{50} of ~15 μM. The effective concentrations of benomyl required to induce the mitotic block in HeLa cells paralleled those required for the inhibition of cell proliferation. Similar to the action of several other antimitotic agents including LY290181, cryptophycin-52, and vinblastine, inhibition of proliferation by benomyl correlated fairly well with the blockage of the cells in mitosis, suggesting that, as in fungal cells, benomyl also blocks HeLa cells in mitosis (*48*, *60*, *61*).

At its half-maximal inhibitory concentration for inhibition of proliferation and mitosis in HeLa cells, benomyl did not depolymerize the microtubules in the cells during interphase, which is similar to the effects of other antimitotic drugs on microtubules during interphase (*48*, *54*). Also, similar to the effects of many other antimitotic drugs on the organization of blocked mitotic spindles, at its lowest effective concentrations (5 μM), benomyl caused little perturbation of spindle microtubule organization (parts C and D of Figure 8). However, small numbers of chromosomes were not aligned properly on the metaphase plate, consistent with the suppression of spindle microtubule dynamics. At high concentrations (e.g., 20 μM), benomyl caused considerable perturbation of spindle microtubule organization and also strongly disrupted the organization of the chromosomes (parts E and F of Figure 8). This is similar to the effects of other more potent antimitotic drugs on the morphology of spindles in blocked cells, indicating that the effects on mammalian spindle organization by benomyl are similar qualitatively to the effects of the more potent microtubule-targeted antimitotic drugs (*48*, *60*, *61*). It is reasonable to think that the inhibitory effects of benomyl on HeLa cell spindle organization and function, like those caused by the more potent antimitotic drugs, are primarily due to the suppression of spindle microtubule dynamics.

In summary, the present paper may explain some of the toxic effects that have been described in mammals and humans for benomyl, such as its teratogenic activity in animals. These findings may also be of value in the design of adjuvant therapy in the treatment of cancer. The rationale is that when used in combination therapy with more potent drugs that act through different mechanisms, weak suppression of spindle microtubule dynamics in tumor cells by low doses of benomyl could contribute to the antitumor activity of the drug combination in the absence of benomyl-induced toxicity.

ACKNOWLEDGMENT

We wish to thank Manas Santra and Tushar Beuria for critical reading of the paper and Herb Miller for providing bovine brain tubulin.

REFERENCES

1. Actor, P., Anderson, E. L., Dicuollo, C. J., Ferlauto, R. J., Hoover, J. R. E., Pagano, J. F., Ravin, L. R., Scheidy, S. F., Stedman, R. J., and Theodorides, V. J. (1967) A new broad spectrum anthelmintic, methyl 5(6)-butyl-2-benzimidazole carbamate, *Nature 215*, 321−322.
2. Hoyt, M. A., Totis, L., and Roberts, B. T. (1991) *S. cerevisiae* genes required for cell cycle arrest in response to loss of microtubule function, *Cell 66*, 507−517.
3. Li, R., and Murray, A. W. (1991) Feedback control of mitosis in budding yeast, *Cell 66*, 519−531.
4. Davidse, L. C., and Flach, W. (1977) Differential binding of methyl benzimidazol-2-yl carbamate to fungal tubulin as a mechanism of resistance to this antimitotic agent in mutant strains of *Aspergillus nidulans*, *J. Cell Biol. 72*, 174−193.
5. Friedman, P. A., and Platzer, E. G. (1978) Interaction of anthelmintic benzimidazoles and benzimidazole derivatives with bovine brain tubulin, *Biochim. Biophys. Acta 544*, 605−614.
6. Friedman, P. A., and Platzer, E. G. (1980) Interaction of anthelmintic benzimidazoles with Ascaris suum embryonic tubulin, *Biochim. Biophys. Acta 630*, 271−278.
7. Kilmartin, J. V. (1981) Purification of yeast tubulin by self-assembly in vitro, *Biochemistry 20*, 3629−3633.
8. Yoon, Y., and Oakley, B. R. (1995) Purification and characterization of assembly competent tubulin from *Aspergillus nidulans*, *Biochemistry 34*, 6373−6381.
9. Downing, K. H. (2000) Structural basis for the interaction of tubulin with proteins and drugs that affect microtubule dynamics, *Annu. Rev. Cell Biol. 16*, 89−111.
10. Downing, K. H. (2000) Structural basis for the action of drugs that affect microtubule dynamics, *Emerging Ther. Targets 4*, 219−237.
11. Richards, K. L., Anders, K. R., Nogales, E., Schwartz, K., Downing, K. H., and Botstein, D. (2000) Structure−function relationships in yeast tubulins, *Mol. Biol. Cell 11*, 1887−1903.
12. Jung, M. K., and Oakley, B. R. (1990) Identification of an amino acid substitution in the benA, β-tubulin gene of *Aspergillus nidulans* that confers thiabendazole resistance and benomyl supersensitivity, *Cell Motil. Cytoskeleton 17*, 87−94.
13. Farr, G. W., and Sternlicht, H. (1992) Site-directed mutagenesis of the GTP-binding domain of β tubulin, *J. Mol. Biol. 227*, 307−321.
14. Jung, M. K., Wilder, I. B., and Oakley, B. R. (1992) Amino acid alterations in the benA (β-tubulin) gene of *Aspergillus nidulans* that confer benomyl resistance, *Cell Motil. Cytoskeleton 22*, 170−174.
15. Reijo, R. A., Cooper, E. M., Beagle, G. J., and Huffaker, T. C. (1994) Systematic mutational analysis of the yeast β-tubulin gene. *Mol. Biol. Cell 5*, 29−43.
16. Machin, N. A., Lee, J. M., and Barnes, G. (1995) Microtubule stability in budding yeast: characterization and dosage suppression of a benomyl-dependent tubulin mutant, *Mol. Biol. Cell 6*, 1241−1259.
17. Li, J., Katiyar, S. K., and Edlind, T. D. (1996) Site-directed mutagenesis of *Saccharomyces cerevisiae* β-tubulin: interaction between residue 167 and benzimidazole compounds, *FEBS Lett. 385*, 7−10.
18. Hollomon, D. W., Butters, J. A., Barker, H., and Hall, L. (1998) Fungal β-tubulin, expressed as a fusion protein, binds benzimi-

dazole and phenylcarbamate fungicides, *Antimicrob. Agents Chemother. 42*, 2171−2173.
19. Gupta, M. L. Jr., Bode, C. J., Dougherty, C. A., Marquez, R. T., and Himes, R. H. (2001) Mutagenesis of β-tubulin cysteine residues in *Saccharomyces cerevisiae*: mutation of cysteine 354 results in cold-stable microtubules, *Cell Motil. Cytoskeleton 49*, 67−77.
20. Lodish, H., Baltimore, D., Berk, A., Zipursky, S. L., Matsudaira, P., and Darnell, J. (1999) *Molecular Cell Biology*, W. H. Freeman, New York.
21. Nogales, E., Wolf, S. G., and Downing, K. H. (1998) Structure of the α and β tubulin dimer by electron crystallography, *Nature 391*, 199−203.
22. Downing, K. H., and Nogales, E. (1998) Tubulin and microtubule structure, *Curr. Opin. Cell Biol. 10*, 16−22.
23. Kirschner, M., and Mitchison, T. (1986) Beyond self-assembly: from microtubules to morphogenesis, *Cell 45*, 329−342.
24. Desai, A., and Mitchison, T. J. (1997) Microtubule polymerization dynamics, *Annu. Rev. Cell Biol. 13*, 83−117.
25. Wilson, L., and Jordan, M. A. (1995) Microtubule dynamics: taking aim at a moving target, *Chem. Biol. 2*, 569−573.
26. Jordan, M. A., and Wilson, L. (1998) Microtubules and actin filaments: dynamic targets for cancer chemotherapy, *Curr. Opin. Cell Biol. 10*, 123−130.
27. Wilson, L., Panda, D., and Jordan, M. A. (1999) Modulation of microtubule dynamics by drugs: A paradigm for the actions of cellular regulators, *Cell Struct. Funct. 24*, 329−335.
28. Jordan, M. A. (2002) Mechanism of action of antitumor drugs that interact with microtubules and tubulin, *Curr. Med. Chem. 2*, 1−17.
29. Hamel, E. (1996) Antimitotic natural products and their interactions with tubulin, *Med. Res. Rev. 16*, 207−231.
30. Uppuluri, S., Knipling, L., Sackett, D. L., and Wolff, J. (1993) Localization of the colchicine-binding site of tubulin, *Proc. Natl. Acad. Sci. U.S.A. 90*, 11598−11602.
31. Bai, R., Pei, X. F., Boye, O., Getahun, Z., Grover, S., Bekisz, J., Nguyen, N. Y., Brossi, A., and Hamel, E. (1996) Identification of cysteine 354 of β-tubulin as part of the binding site for the A ring of colchicine, *J. Biol. Chem. 271*, 12639−12645.
32. Bai, R. L., Pettit, G. R., and Hamel, E. (1990) Binding of dolastatin 10 to tubulin at a distinct site for peptide antimitotic agents near the exchangeable nucleotide and vinca alkaloid sites, *J. Biol. Chem. 265*, 17141−17149.
33. Rai, S. S., and Wolff, J. (1996) Localization of the vinblastine-binding site on β-tubulin, *J. Biol. Chem. 271*, 14707−14711.
34. Cleveland, D. W., and Sullivan, K. F. (1985) Molecular biology and genetics of tubulin, *Annu. Rev. Biochem. 54*, 331−365.
35. Neff, N. F., Thomas, J. H., Grisafi, P., and Botstein, D. (1983) Isolation of the β-tubulin gene from yeast and demonstration of its essential function in vivo, *Cell 33*, 211−219.
36. Hamel, E., and Lin, C. M. (1981) Glutamate-induced polymerization of tubulin: characteristics of the reaction and application to the large-scale purification of tubulin, *Arch. Biochem. Biophys. 209*, 29−40.
37. Panda, D., Chakrabarti, G., Hudson, J., Pigg, K., Miller, H. P., Wilson, L., and Himes, R. H. (2000) Suppression of microtubule dynamic instability and treadmilling by deuterium oxide, *Biochemistry 39*, 5075−5081.
38. Bradford, M. M. (1976) A rapid and sensitive method for the quantitation of microgram quantities of protein utilizing the principle of protein-dye binding, *Anal. Biochem. 72*, 248−254.
39. Gaskin, F., Cantor, C. R., and Shelanski, M. L. (1974) Turbidimetric studies of the in vitro assembly and disassembly of porcine neurotubules, *J. Mol. Biol. 89*, 737−755.
40. Bhattacharyya, B., and Wolff, J. (1975) The interaction of 1-anilino-8-naphthalene sulfonate with tubulin: a site independent of the colchicine-binding site, *Arch. Biochem. Biophys. 167*, 264−269.
41. Lakowicz, J. R. (1999) *Principles of Fluorescence Spectroscopy*, 2nd ed., Kluwer Academic/Plenum Publishers, New York.
42. Ward, L. D. (1985) Measurement of ligand binding to proteins by fluorescence spectroscopy, *Methods Enzymol. 117*, 509−525.
43. Bhattacharyya, B., and Wolff, J. (1974) Promotion of fluorescence upon binding of colchicine to tubulin, *Proc. Natl. Acad. Sci. U.S.A. 71*, 2627−2631.
44. Ellmann, G. L. (1959) Tissue sulfhydryl groups, *Arch. Biochem. Biophys. 82*, 70−77.
45. Panda, D., Daijo, J. E., Jordan, M. A., and Wilson, L. (1995) Kinetic stabilization of microtubule dynamics at steady state in vitro by substoichiometric concentrations of tubulin-colchicine complex, *Biochemistry 34*, 9921−9929.
46. Panda, D., Samuel, J. C., Massie, M., Feinstein, S. C., and Wilson, L. (2003) Differential regulation of microtubule dynamics by three- and four-repeat τ: implications for the onset of neurodegenerative disease, *Proc. Natl. Acad. Sci. U.S.A. 100*, 9548−9553.
47. Skehan, P., Storeng, R., Scudiero, D., Monks, A., McMahon, J., Vistica, D., Warren, J. T., Bokesch, H., Kenney, S., and Boyd, M. R. (1990) New colorimetric cytotoxicity assay for anticancer-drug screening, *J. Natl. Cancer Inst. 82*, 1107−12.
48. Jordan, M. A., Thrower, D., and Wilson, L. (1991) Mechanism of inhibition of cell proliferation by Vinca alkaloids, *Cancer Res. 51*, 2212−2222.
49. Huang, S. C., and Lee, T. C. (1998) Arsenite inhibits mitotic division and perturbs spindle dynamics in HeLa S3 cells, *Carcinogenesis 19*, 889−896.
50. Wilson, L. (1970) Properties of colchicine binding protein from chick embryo brain. Interactions with vinca alkaloids and podophyllotoxin, *Biochemistry 9*, 4999−5007.
51. Kuriyama, R., and Sakai, H. (1974) Role of tubulin-SH groups in polymerization to microtubules. Functional-SH groups in tubulin for polymerization, *J. Biochem. 81*, 1115−1125.
52. Luduena, R. F., and Roach, M. C. (1991) Tubulin sulfhydryl groups as probes and targets for antimitotic and antimicrotubule agents, *Pharmacol. Ther. 49*, 133−152.
53. Roychowdhury, M., Sarkar, N., Manna, T., Bhattacharyya, S., Sarkar, T., Basusarkar, P., Roy, S., and Bhattacharyya, B. (2000) Sulfhydryls of tubulin: A probe to detect conformational changes of tubulin, *Eur. J. Biochem. 267*, 3469−3476.
54. Jordan, M. A., Thrower, D., and Wilson, L. (1992) Effects of vinblastine, podophyllotoxin and nocodazole on mitotic spindles. Implications for the role of microtubule dynamics in mitosis, *J. Cell Sci. 102*, 401−416.
55. Urani, C., Chiesara, E., Galvani, P., Marabini, L., Santagostino, A., and Camatini, M. (1995) Benomyl affects the microtubule cytoskeleton and the glutathione level of mammalian primary cultured hepatocytes, *Toxicol. Lett. 76*, 135−144.
56. Margolis, R. L., and Wilson, L. (1977) Addition of colchicine−tubulin complex to microtubule ends: the mechanism of substoichiometric colchicine poisoning, *Proc. Natl. Acad. Sci. U.S.A. 74*, 3466−3470.
57. Skoufias, D. A., and Wilson, L. (1992) Mechanism of inhibition of microtubule polymerization by colchicine: inhibitory potencies of unliganded colchicine and tubulin−colchicine complexes, *Biochemistry 31*, 738−746.
58. Sternlicht, H., and Ringel, I. (1979) Colchicine inhibition of microtubule assembly via copolymer formation, *J. Biol. Chem. 254*, 10540−10550.
59. Jordan, M. A., and Wilson, L. (1990) Kinetic analysis of tubulin exchange at microtubule ends at low vinblastine concentrations, *Biochemistry 29*, 2730−2739.
60. Panda, D., DeLuca, K., Williams, D., Jordan, M. A., and Wilson, L. (1998) Antiproliferative mechanism of action of cryptophycin-52: kinetic stabilization of microtubule dynamics by high-affinity binding to microtubule ends, *Proc. Natl. Acad. Sci. U.S.A. 95*, 9313−9318.
61. Panda, D., Singh, J. P., and Wilson, L. (1997) Suppression of microtubule dynamics by LY290181. A potential mechanism for its antiproliferative action, *J. Biol. Chem. 272*, 7681−7687.

BI036112V